The effect of X-ray scanning on intensity and binding energy of photoelectron peak and the line scanning analysis of an etched crater

Michiko Yoshitake and Kazuhiro Yoshihara

National Research Institute for Metals

(Received October 7 1998; accepted January 18 1999)

The effect of X-ray scanning on the intensity and binding energy distribution in XPS was examined prior to the line scanning analysis of layered specimens. No distribution in both intensity and binding energy was found in non-dispersive direction but meaningful distribution in dispersive direction. Layered intermetallic compounds formed by annealing a Ti film on a Cu substrate and a Nb film on Ti substrate were characterized by line scan analysis across an etched crater. The intensity profile along the line clearly showed plateaus corresponding to each compound layer for both specimens. The binding energy at each plateau clearly showed the chemical shifts upon the formation of intermetallic compounds. The comparison between the thickness obtained by line scanning and stylus profile and that obtained by sputter depth profile showed that the line scanning can give more accurate thickness when the sputtering rate among layers varies. It was shown that the line profiling technique with a scanning XPS enables simultaneous analysis of the composition and the chemical state of layered materials as thick as sub-micrometer.

1. Introduction

X-ray photoelectron spectroscopy (XPS) is a helpful tool for wide range of material characterization. Especially the ability of mapping chemical state is the advantage of spatially resolved XPS. The development of spatially resolved XPS is remarkable and a scanning XPS instrument enables us chemical state mapping in the way scanning AES did element mapping years ago or so. This paper represents some basic features of a scanning XPS to show the usefulness of line profile analysis of layered material.

2. Experiment

A scanning X-ray photoelectron spectrometer (PHI Quantum 2000) was used for the measurement. It uses focused Al K α X-ray monocromatized by quartz crystals. Quartz crystals are aligned with two-dimensional curvature so that the area of X-ray generation is projected on a specimen[1]. X-ray beam of 10 $\mu m \phi$ in size with 20 W was used for this study. The reproducibility of binding energy was within $\pm$0.03 eV.

The intensity and the binding energy of Cu $2p_{3/2}$ on pure Cu are measured by scanning 2000μm range in non-dispersive and dispersive directions to check lateral distribution of signal. As a reference, measurement was done by moving the specimen stage $\pm$ 800μm so that the measurement was always done at the center position of the instrument (optimum position without scanning) but different points on the specimen.

Two specimens, Ti film deposited on Cu substrate and Nb film deposited on Ti substrate, which were heated in a vacuum after deposition, were analyzed. Three kinds of intermetallic compounds, γ-TiCu, Ti_3Cu_4 and $TiCu_3$ identified by X-ray diffraction existed in the Ti-Cu specimen. No evident intermatallic compounds were found in Nb-Ti specimen by X-ray diffraction. Both film were sputter etched by 2kV Ar ion and etched craters were made for analysis. To convert the distance in line profile into the depth, the etched craters were traced with a stylus.

3. Intensity and binding energy distribution on Cu

Intensity distributions of Cu $2p_{3/2}$ in non-dispersive direction and dispersive direction measured with pass energy 46 eV are plotted in Fig.1. Intensity was calculated by area which ranged (peak energy $\pm$5.0 eV) so that whole peak area was included. In non-dispersive direction, the intensity is almost constant over $\pm$600μm. In dispersive direction, the intensity drops significantly as the measurement position is away from the center point. To confirm that the above distribution is caused by X-ray scan but not by inhomogeneity of a specimen, intensity

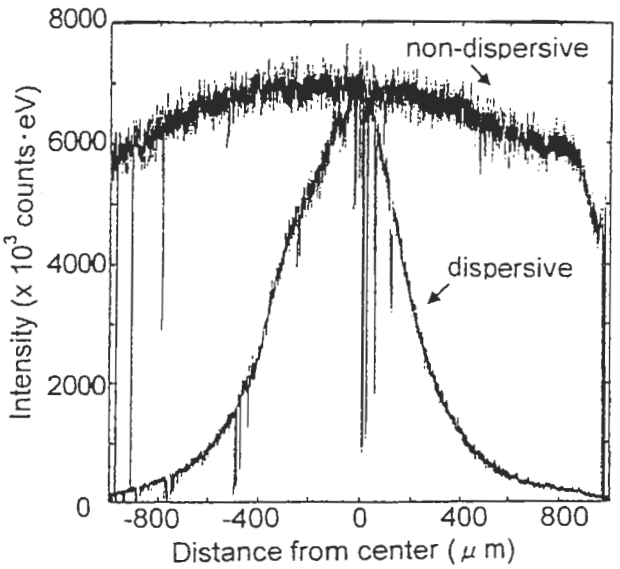

Fig.1 Intensity distribution of Cu $2p_{3/2}$ in scan mode.

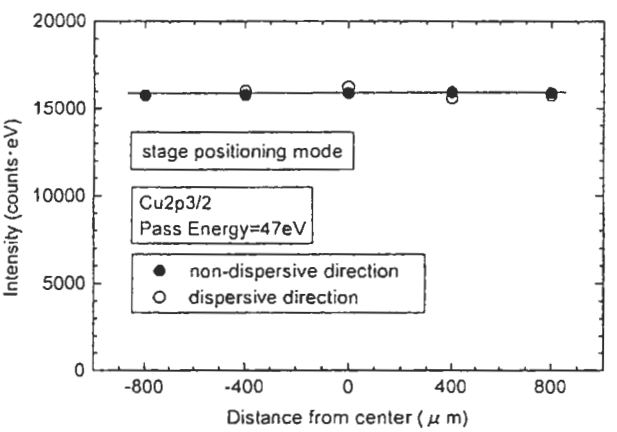

Fig.2 Intensity distribution of Cu $2p_{3/2}$ in stage positioning mode.

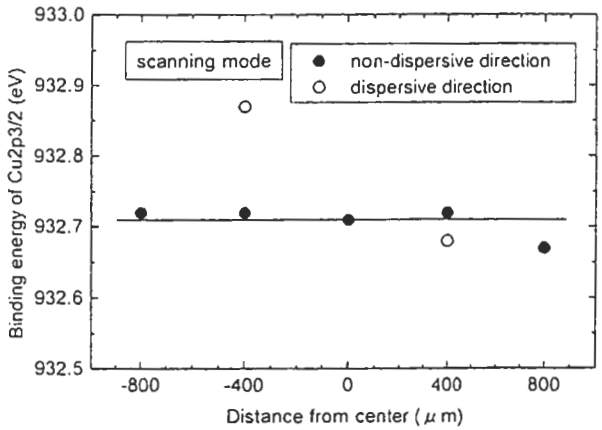

Fig.3 Binding energy distribution of Cu $2p_{3/2}$ in scan mode.

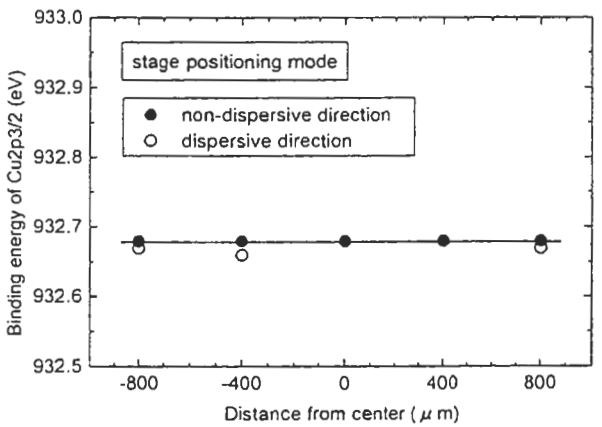

Fig.4 Binding energy distribution of Cu $2p_{3/2}$ in stage positioning mode.

distribution of Cu $2p_{3/2}$ at several positions on the specimen is measured by positioning the specimen stage in non-dispersive and dispersive directions. The results are shown in Fig.2. On the same specimen as in Fig.1, there is no intensity deviation for both directions. Therefore, the intensity distribution shown in Fig.1 is caused by X-ray scanning. In Fig.1, the effect of the energy change of X-ray irradiating a specimen is also included in the intensity distribution of dispersive direction. Therefore, the shape shown in Fig.1 is not symmetrical because of asymmetrical energy distribution of generated X-ray itself.

The above results show that line profile analysis of a specimen by scanning XPS should be done in non-dispersive direction and when intensity mapping is applied one must be careful that obtained data include the effect of X-ray intensity distribution on a specimen.

The binding energy of Cu $2p_{3/2}$ in non-dispersive direction and dispersive direction measured by scanning X-ray is plotted in Fig3. In non-dispersive direction, binding energy only deviates 0.02eV, which is within the limit of repeatability. In contrast to this, meaningful deviation was observed in dispersive direction. As a reference, binding energy on the same positions of the specimen was measured by positioning a specimen stage. As shown in Fig.4, the binding energy is same within the limit of repeatability.

Therefore, line profile analysis of a specimen by scanning XPS should be done in non-dispersive direction and the effect of X-ray scanning should be in mind when chemical mapping is applied.

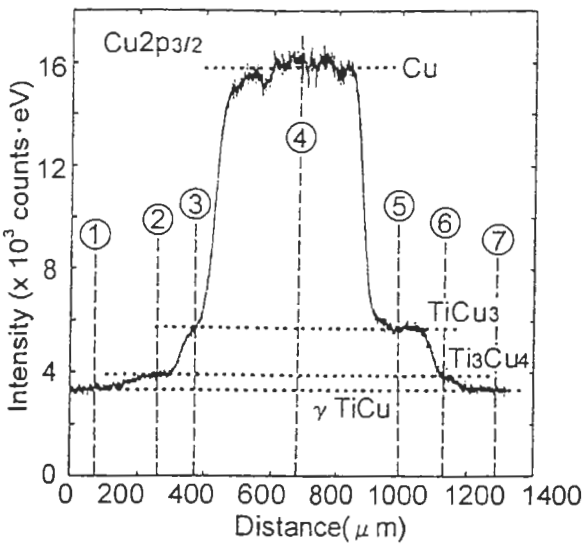

Fig.5 Intensity line profile of Cu $2p_{3/2}$ for the non-dispersive direction in Ti-Cu specimen.

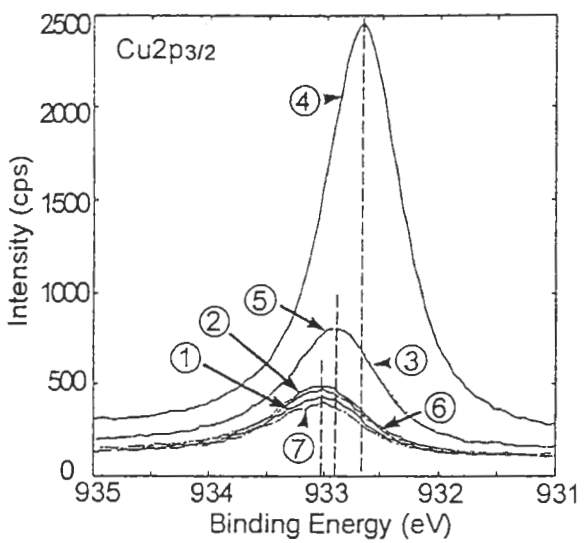

Fig.6 XPS spectra of Cu $2p_{3/2}$ at plateaus in Fig.5.

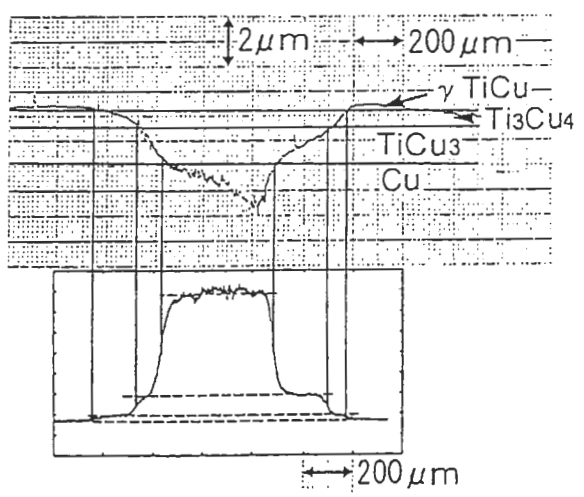

Fig.7 Stylus profile of the crater on Ti-Cu specimen with intensity profile shown in Fig.5.

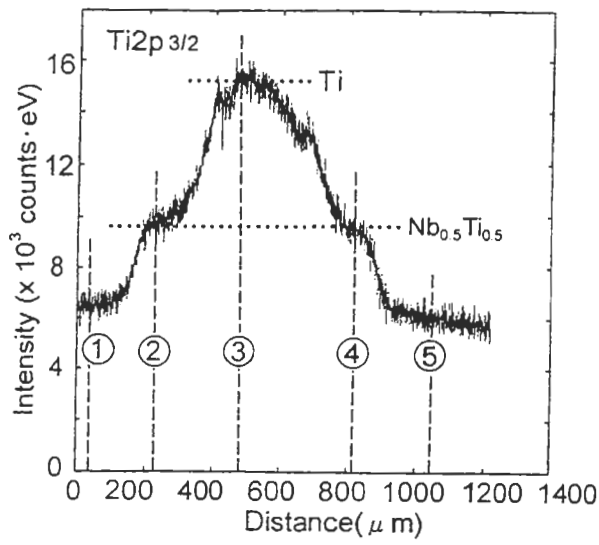

Fig.8 Intensity line profile of Ti $2p_{3/2}$ for the non-dispersive direction in Nb-Ti specimen.

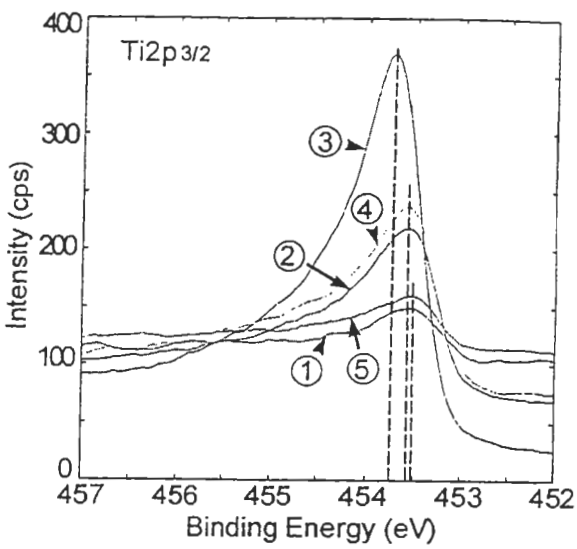

Fig.9 XPS spectra of Ti $2p_{3/2}$ at plateaus in Fig.8.

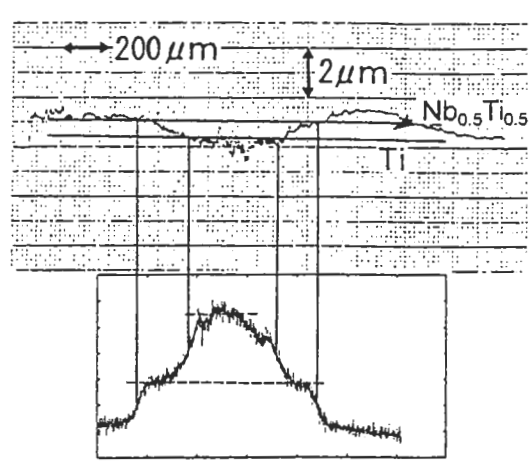

Fig.10 Stylus profile of the crater on Nb-Ti specimen with intensity profile shown in Fig.8.

4. Line profile of layered materials

The photoelectron intensity and the binding energy along a line that crosses an etched crater were measured. Fig.5 shows the intensity line profile of Ti-Cu specimen. Each plateau in Fig.5 is attributed to γ-TiCu, Ti_3Cu_4, $TiCu_3$, or Cu according to its order in intensity. Figure 6 shows the XPS spectra of Cu $2p_{3/2}$ at several points indicated in Fig.5. The binding energy shifts to higher value by the formation of intermetallic compounds. The binding energy differences among intermetallic compounds are also observed. The stylus profile of the crater is shown in Fig.7 together with the intensity line profile of Cu $2p_{3/2}$. From the comparison between the stylus profile and the intensity line profile, the thickness of each intermetallic compound are estimated to be 0.3μm for γ-TiCu, 0.7μm for Ti_3Cu_4, and 1.2μm for $TiCu_3$, respectively. The thickness of each layer obtained by the AES sputter depth profile was 0.6μm, 0.7μm and 1.0μm, respectively[2]. It is very likely that the thickness calculated from a sputter depth profile gives larger value for Ti rich intermetallic compounds, as the sputtering rate of pure Ti is three times smaller that that of pure Cu[3].

Figure 8 shows the intensity line profile of Nb-Ti specimen. There is a plateau at the composition of $Nb_{0.5}Ti_{0.5}$ which was also observed in AES sputter depth profile[4]. Figure 9 shows the XPS spectra of $Ti2p_{3/2}$ at several points indicated in Fig.8. The binding energy of $Ti2p_{3/2}$ at $Nb_{0.5}Ti_{0.5}$ composition shows chemical shift. The stylus profile of the crater is shown in Fig.10 together with the intensity line profile of $Ti2p_{3/2}$. From the comparison between the stylus profile and the intensity line profile, the depth and the thickness of $Nb_{0.5}Ti_{0.5}$ compound are 0.6μm and 0.7μm, respectively. The depth and thickness obtained by the AES sputter depth profile was 0.7μm and 0.8μm respectively[4]. The values obtained with line profile and sputter depth profile are similar in Nb-Ti compound in contrast to Ti-Cu compounds. The reason is considered that the sputtering rate of Nb and Ti is almost the same[3]. Therefore, although the amount of error in the stylus profile is not small, a line profile of the crater will give the reasonable information on the thickness of each layer in addition to the information on composition and chemical state of each layer.

5. Summary

The effect of X-ray scanning on the intensity and binding energy distribution of Cu photoelectron peak was examined prior to the line profile analysis of layered specimens by scanning XPS. It was confirmed that there was no distribution in both intensity and binding energy in non-dispersive direction but meaningful distribution in dispersibe direction.

Layered intermetallic compounds formed by annealing Ti film on Cu substrate and Nb film on Ti substrate were characterized by scanning XPS. The photoelectron intensity and the binding energy were measured across an etched crater. The intensity profile along the line clearly showed plateaus corresponding to each compound layer for both specimens. The binding energy at each plateau clearly showed the chemical shifts upon the formation of intermetallic compounds. The comparison between the thickness obtained by line profile and stylus profile and that obtained by sputter depth profile showed that the line profile can give more accurate thickness when the sputtering rate among layers varies. The line profile technique with scanning XPS enables simultaneous analysis of the composition and the chemical state of layered materials as thin as sub-micrometer.

6. References

[1]H.Iwai, R.Oiwa and M.Kudo; J.Surf.Sci.Soc.Jpn, 17, 406(1996).

[2]M.Yoshitake and K.Yoshihara; J.Japan Inst.Metals, 54, 778(1990).

[3]N.Laegreid and G.K.Wehner; J.Appl.Phys. 32, 365(1961).: D.Rosenberg and G.K.Wehner; J.Appl.Phys. 33, 1842(1962).: R.C.Bradley; Phys.Rev., 93, 719(1954).

[4]M.Yoshitake and K.Yoshihara; J.Japan Inst.Metals, 54, 1013(1990).